AIP | Applied Physics Letters

Evidence for ferromagnetic strain glass in Ni-Co-Mn-Ga Heusler alloy system

Yu Wang, Chonghui Huang, Jinghui Gao, Sen Yang, Xiangdong Ding et al.

Citation: Appl. Phys. Lett. **101**, 101913 (2012); doi: 10.1063/1.4751250
View online: http://dx.doi.org/10.1063/1.4751250
View Table of Contents: http://apl.aip.org/resource/1/APPLAB/v101/i10
Published by the American Institute of Physics.

Evidence for ferromagnetic strain glass in Ni-Co-Mn-Ga Heusler alloy system

Yu Wang,[1,a)] Chonghui Huang,[1] Jinghui Gao,[1] Sen Yang,[1] Xiangdong Ding,[1] Xiaoping Song,[1,b)] and Xiaobing Ren[1,2,c)]
[1]*MOE Key Laboratory for Nonequilibrium Synthesis and Modulation of Condensed Matter and State Key Laboratory for Mechanical Behavior of Materials, Xi'an Jiaotong University, Xi'an 710049, China*
[2]*Multi-Disciplinary Materials Research Center, Frontier Institute of Science and Technology, Xi'an Jiaotong University, Xi'an 710049, China and National Institute for Materials Science, 1-2-1 Sengen, Tsukuba 305-0047, Ibaraki, Japan*

(Received 2 April 2012; accepted 22 August 2012; published online 7 September 2012)

We report that both a strain glass transition and a ferromagnetic transition take place in a $Ni_{43}Co_{12}Mn_{20}Ga_{25}$ Heusler alloy. This results in a ferromagnetic strain glass with coexisting short range strain ordering and long range magnetic moment ordering. The phase diagram of the Ni-Co-Mn-Ga system shows that the substitutional point defect Co in the Ni-site plays the following roles: (i) suppressing the long range strain ordering of martensite, (ii) promoting local strain ordering of strain glass by producing random local stresses, and (iii) enhancing the ferromagnetic exchange interaction, which leads to the formation of ferromagnetic strain glass. © *2012 American Institute of Physics*. [http://dx.doi.org/10.1063/1.4751250]

Martensitic transition is known as a diffusionless structure transition with the formation of long range lattice strain ordering in martensite.[1] This transition results in the shape memory effect and superelastic behavior and makes the martensitic alloys become important functional materials. Among the martensitic alloys family, the Heusler alloys are very unique for showing both martensitic and magnetic transition.[2] Due to the interaction between the strain and magnetic degrees of freedom, Heusler martensitic alloys exhibit multi-functional properties such as magnetic shape memory effect[3,4] and magnetocaloric effect[5] and have attracted intensive investigation for decades.

The composition of martensitic alloys (including Heusler martensitic alloys) are often modified by doping in practice, because the dopant elements (point defects) can affect their transition behavior,[1,6–12] which further alters their functional properties. Recent studies show that doping sufficient defect elements such as Fe, Co, and Cr in to Ti-Ni and Ti-Pd martensitic alloys can suppress the spontaneous martensitic transition[9–12] but lead to the formation of strain glass transition in these systems.[10–14] The formation of long range strain ordering (martensitic twin morphology) was prohibited in strain glass for the existence of point defects, while randomly distributed short range strain ordering (martensitic nano-domain structure) persists and freezes kinetically in strain glass state.[12–14] The strain glass transition does not accompany structure variation.[12,14] However, it is characterized by frequency dependent dynamic mechanical anomalies conforming to the Vogel-Fulcher relationship,[12] which demonstrates the existence of a kinetic freezing transition.

As mentioned above, the martensitic transition and ferromagnetic transition can coexist in the Heusler alloy system, which leads to the ferromagnetic martensite. However, it is unknown so far whether there is a ferromagnetic strain glass in the martensitic-derived system. In this study, we report that the $Ni_{43}Co_{12}Mn_{20}Ga_{25}$ Heusler alloy undergoes a ferromagnetic transition at high temperature and then undergoes a strain glass transition at low temperature. This leads to the formation of a ferromagnetic strain glass state, in which the short range strain ordering and long range magnetic moment ordering coexist. The formation of ferromagnetic strain glass by doping substitutional point defect Co in the Ni-site of Ni-Co-Mn-Ga alloy is also discussed through a phase diagram of the system.

A series of Heusler alloys $Ni_{55-x}Co_xMn_{20}Ga_{25}$ ($x = 0$, 2, 4, 6, 8, 10, 12, 15, 18) were fabricated by arc melting 99.9% pure metals of Ni, Co, Mn, and Ga in argon atmosphere. The as-cast ingots were annealed at 1173 K for 24 h in evacuated quartz tubes and subsequently quenched into room temperature water. To characterize the lattice strain states in the samples, the dynamic mechanical analysis (DMA) was performed in a DMA Q800 from TA Instruments. To identify the magnetic states of these samples, the temperature dependence of magnetization was performed with a LakeShore 7300 vibrating sample magnetometer (VSM). The transition latent heat was measured by a differential scanning calorimeter (DSC) of Q100 from TA Instruments. Moreover, *in situ* x-ray diffraction (XRD) measurement was also performed on bulk samples in a Bruker x-ray diffractometer to monitor their structure evolution upon temperature. The microscopic observation was done in a JEOL JEM-2100 transmission electron microscope to explore the microstructure of the strain glass sample.

The ferromagnetic strain glass was obtained by doping sufficient Co into the Ni-site of $Ni_{55}Mn_{20}Ga_{25}$ Heusler martensitic alloy. In the following, we will first display the transition behavior of the pure $Ni_{55}Mn_{20}Ga_{25}$ martensitic terminal and then show how the transforming properties of the system change as a function of defect (Co) concentration. The typical transforming behavior of $Ni_{55}Mn_{20}Ga_{25}$ magnetic martensitic alloy is shown in Fig. 1. Its dynamic mechanical analysis (Fig. 1(b)) displays a sharp modulus dip with insignificant frequency dispersion in its dip temperature, which is the typical characteristic of martensitic

[a)]Electronic mail: yuwang@mail.xjtu.edu.cn.
[b)]Electronic mail: songxp@mail.xjtu.edu.cn.
[c)]Electronic mail: REN.Xiaobing@nims.go.jp.

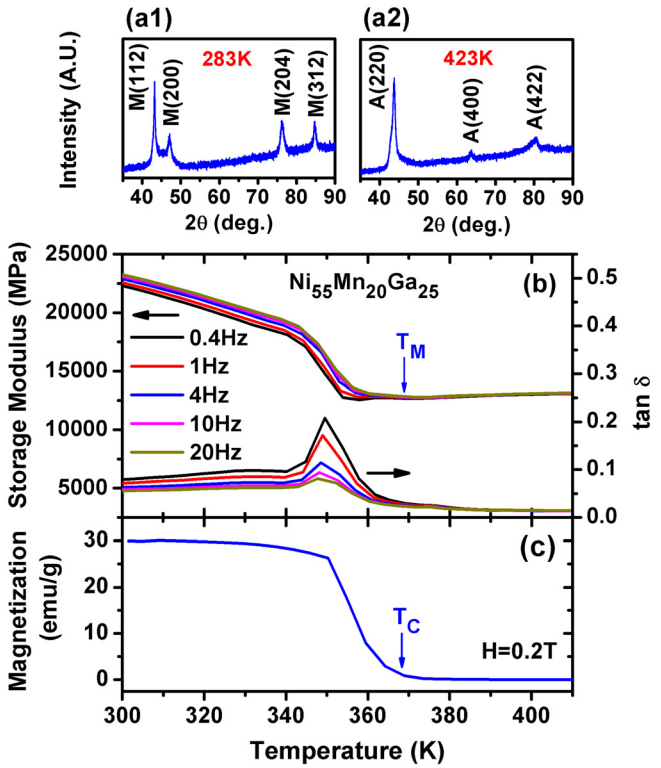

FIG. 1. The transforming behaviors of $Ni_{55}Mn_{20}Ga_{25}$ ferromagnetic martensitic alloy. The XRD profiles of (a1) $L2_1$ austenite (423 K) and (a2) tetragonal martensite (283 K) for this alloy. (b) The dynamic mechanical properties of the sample. (c) The magnetization vs. temperature curve measured under the magnetic field of 0.2 T for the sample.

transition.[15,16] The XRD profiles in Figs. 1(a1) and 1(a2) demonstrate that its martensitic transition accompanies the structure change from $L2_1$ austenite (423 K) to tetragonal martensite (283 K). Moreover, a ferromagnetic transition was detected by the temperature dependence of magnetization in Fig. 1(c). The martensitic transition temperature T_M (369 K) of $Ni_{55}Mn_{20}Ga_{25}$ coincides with its Curie temperature T_C (368 K), revealing the simultaneous formation of long range strain and magnetic moment order in the sample.

The transition behavior of $Ni_{55-x}Co_xMn_{20}Ga_{25}$ ($x = 0$–18) alloys changes greatly with increasing Co doping, which is well revealed by the comparison of their DSC curves in Fig. 2. As shown in Figs. 2(a)–2(c), the exothermal/endothermic peaks of $Ni_{55-x}Co_xMn_{20}Ga_{25}$ ($x = 0$, 4, 8) alloys exhibit the jerky characteristic, which is well-known for the Ni-Mn-Ga based martensitic Heusler alloys.[7] The jerky characteristic of DSC peak is caused by successive sudden progression of big austenite/martensite phase boundary during martensitic transition,[17,18] the appearance of which is very sensitive to diverse factors such as disorder, composition, and heat treatment.[17] Thus, it may appear in some Ni-Mn-Ga alloys,[7] while it may not be observed in others with different disorder, composition, or heat treatment.[19] With the increase of Co content x, the martensitic transition temperature (T_M) of $Ni_{55-x}Co_x$ $Mn_{20}Ga_{25}$ sample shows slight change when $x \leq 4$ but exhibits a rapid drop when $4 < x \leq 8$ (Fig. 2(e)). This reflects that the martensitic stability was reduced greatly by the substitutional doping of Co into the Ni-site of this system. The corresponding transition latent heat obtained from both cooling and heating processes decreases rapidly when x

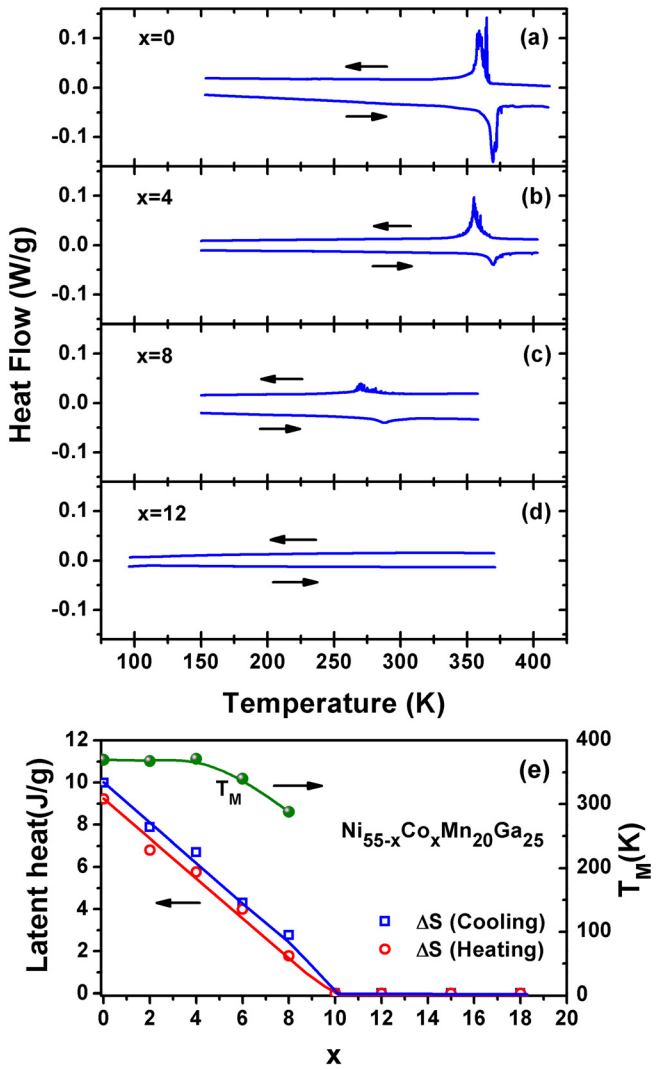

FIG. 2. The change of the transforming signatures of the $Ni_{55-x}Co_xMn_{20}Ga_{25}$ ($x = 0$–18) alloys with increasing Co doping. (a)-(d) show the DSC curves of $Ni_{55-x}Co_xMn_{20}Ga_{25}$ ($x = 0$, 4, 8, 12) alloys respectively. (e) The change of the transition latent heat (ΔS) and the martensitic transition temperature (T_M) of $Ni_{55-x}Co_xMn_{20}Ga_{25}$ ($x = 0$–18) samples as a function of Co content (x).

increases from 0 to 8, as shown in Fig. 2(e). More interestingly, the transition latent heat of $Ni_{55-x}Co_xMn_{20}Ga_{25}$ samples vanishes when $x \geq 10$ (Fig. 2(e)), as exampled by the absence of exothermal/endothermic peaks in the DSC curve of Ni_{43} $Co_{12}Mn_{20}Ga_{25}$ sample in Fig. 2(d). This suggests the absence of martensitic transition at high Co doping regime ($x \geq 10$). The reduction of martensitic transition temperature and the weakening of the transition signature by doping defects in the Ni-Co-Mn-Ga system are similar to those observed in the defect doped Ti-Ni and Ti-Pd system. This indicates that strain glass transition likely appears in the heavily doped $Ni_{55-x}Co_xMn_{20}Ga_{25}$ samples.

Fig. 3 shows the experimental evidence for the strain glass transition in $Ni_{43}Co_{12}Mn_{20}Ga_{25}$ Heusler alloys. As displayed in Figs. 3(a1)-3(a3), the XRD profiles of the samples do not show any macroscopic crystal symmetry change from 313 K to 170 K, indicating no structure transition occurs in this temperature range. This is consistent with the disappearance of exothermal/endothermic peak in its DSC curve in Fig. 2(d). However, its DMA results (Fig. 3(b)) exhibit a

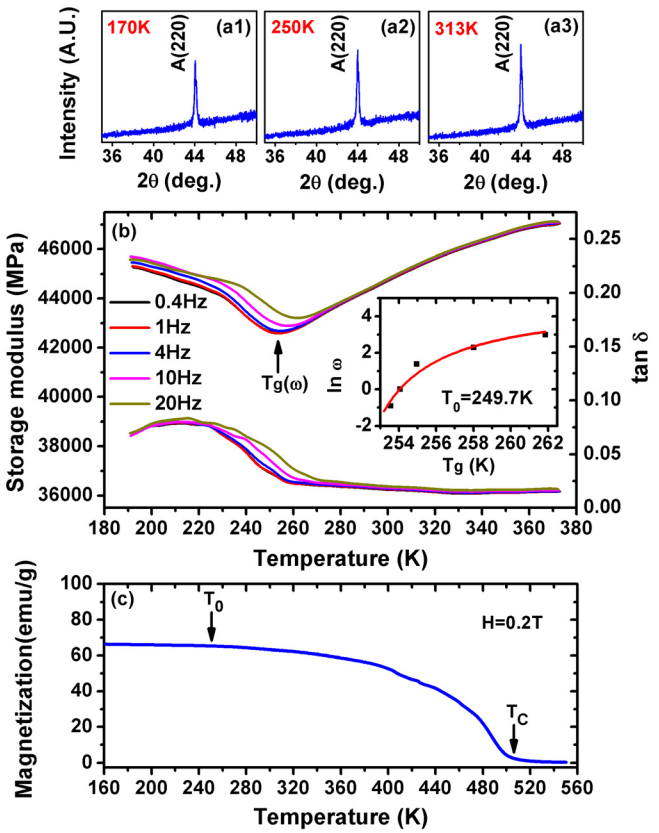

FIG. 3. The experimental evidence for the ferromagnetic strain glass in $Ni_{43}Co_{12}Mn_{20}Ga_{25}$ Heusler alloy. (a1)–(a3) show the XRD profiles of the sample measured at 170 K, 250 K, and 313 K, respectively. (b) The dynamic mechanical properties of $Ni_{43}Co_{12}Mn_{20}Ga_{25}$ ferromagnetic strain glass. The inset shows that the frequency (ω) dispersion behavior of its storage modulus dip temperature ($T_g(\omega)$) conforms to the Vogel-Fulcher relationship. (c) The magnetization vs. temperature curve measured under the magnetic field of 0.2 T for the sample.

broad storage modulus dip in this temperature regime, which indicates the existence of a transition. Moreover, the frequency (ω) dispersion of its storage modulus dip temperature ($T_g(\omega)$) obeys the Vogel-Fulcher relationship $\omega = \omega_0 \exp[-E_a/k_B(T_g(\omega) - T_0)]$ (inset of Fig. 3(b)). This is the typical freezing feature of strain glass,[12] demonstrating the strain glass transition does exist in $Ni_{43}Co_{12}Mn_{20}Ga_{25}$ Heusler alloys. Its ideal freezing temperature T_0 yields 249.7 K by fitting the frequency dependent modulus dip temperatures with the Vogel-Fulcher relationship. Notably, the temperature dependence of magnetization of this strain glass alloy shows a ferromagnetic transition at the Curie temperature T_C of 506 K (Fig. 3(c)), being much higher than its ideal freezing temperature T_0. This demonstrates that there exists a ferromagnetic strain glass with the coexistence of short range strain ordering and long range magnetic moment ordering.

The martensitic nano-domain structure of the ferromagnetic strain glass $Ni_{43}Co_{12}Mn_{20}Ga_{25}$ was observed by transmission electron microscopy at room temperature. As shown by the bright field image in Fig. 4, no martensitic variant plates and twin morphology appear in the sample, but many nano-domains with the size of 10 nm–40 nm exist. The corresponding electron diffraction pattern taken from the $[1\ 0\ 0]_A$ zone axis of austenite structure shows a $L2_1$ reflections, being consistent with XRD measurement. However, some

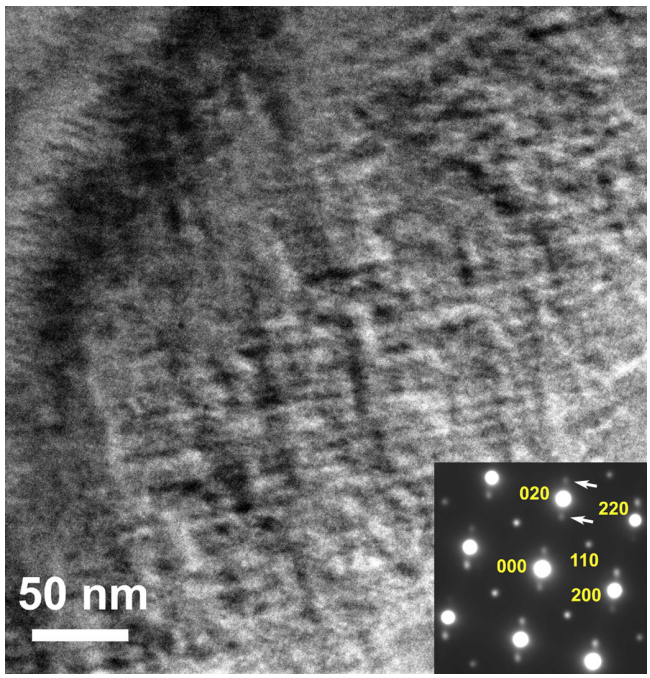

FIG. 4. Bright field image of the ferromagnetic strain glass $Ni_{43}Co_{12}Mn_{20}Ga_{25}$. The inset shows the corresponding electron diffraction pattern of $[1\ 0\ 0]_A$ zone axis of austenite structure.

weak and diffuse reflections (indicated by white arrows in the inset of Fig. 4) appear near the main diffraction spots, which resemble the corresponding diffraction spots for the tetragonal martensite of Ni-Mn-Ga martensitic alloy.[20] This indicates that the nano-domains possess local tetragonal lattices. It should be mentioned that the size of the ferromagnetic domains of ferromagnetic martensitic alloy is in micrometer scale as reported previously,[21,22] which is much bigger than the martensitic nano-domains of ferromagnetic strain glass.

The evolution of the lattice strain state and magnetic state as a function of Co content x and electron concentration e/a of $Ni_{55-x}Co_xMn_{20}Ga_{25}$ system is displayed in the phase diagram of Fig. 5, which well reveals the formation of ferromagnetic strain glass by doping point defects. The martensitic transition temperatures T_M in the phase diagram were obtained by DSC and DMA measurements and the ferromagnetic transition temperatures T_C were determined by magnetization vs. temperature curves. As shown in Fig. 5, when the composition of $Ni_{55-x}Co_xMn_{20}Ga_{25}$ $(0 \le x \le 2)$ system is close to its pure $Ni_{55}Mn_{20}Ga_{25}$ martensitic terminal, the martensitic transition of the system coincides with its ferromagnetic transition. In addition, both the martensitic and ferromagnetic transition temperatures show insignificant change with the increase of Co content. The system transforms from the paramagnetic austenite into the ferromagnetic martensite upon cooling.

The martensitic transition temperature T_M starts to decrease rapidly on further increasing the Co content up to a critical value x_c, while the ferromagnetic transition temperature T_C increases rapidly with increasing Co doping. Thus, the system first transforms from the paramagnetic austenite into the ferromagnetic austenite at high temperature and then into the ferromagnetic martensite at low temperature. The reduction of T_M demonstrates that the stability of martensite is greatly reduced by doping substitutional point defect Co

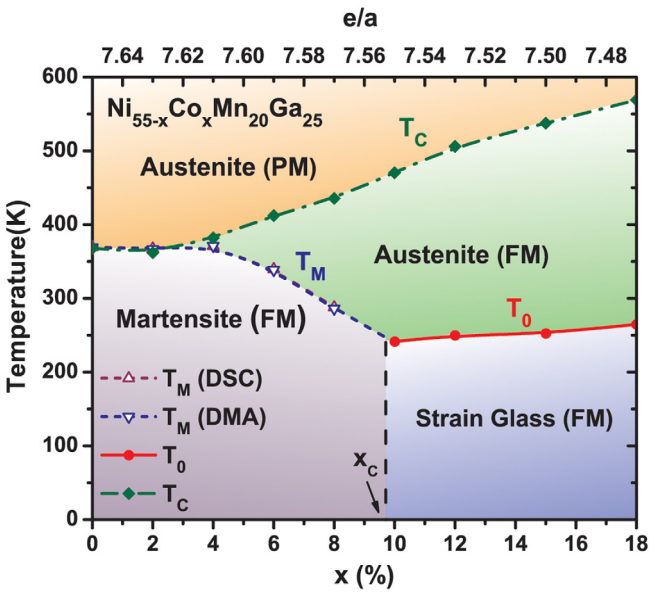

FIG. 5. The phase diagram of $Ni_{55-x}Co_xMn_{20}Ga_{25}$ Heusler system. It displays the evolution of the lattice strain state and magnetic state as a function of Co content (x) and electron concentration (e/a) of the system. The PM and FM in the figure stand for the paramagnetic and ferromagnetic state, respectively.

into the Ni-site. This fact is consistent with previous studies of the doping effect in Ni-Mn-Ga Heusler system.[7,8] It was considered that the decrease of T_M stems from the decrease of the electron concentration e/a by the replacing Ni with Co.[7] The increase of the T_C is suggested to relate with the higher magnetic moment of Co than that of Ni and stronger exchange interaction of Co-Mn as compared with Ni-Mn.[8]

When the Co content is above the critical value x_c, the martensitic transition of the system is completely suppressed and replaced by the strain glass transition. However, the ferromagnetic transition temperature T_C increases further to higher temperature with increasing Co doping. Upon cooling, the system first transforms from the paramagnetic austenite to ferromagnetic austenite (unfrozen state) and then into the ferromagnetic strain glass (frozen state). Previous study[23] shows that the doped point defect should satisfy two conditions in order to generate strain glass in the martensitic-derived system. First, it decreases the thermodynamic driving force for forming long range strain order, i.e., it reduces the phase stability of martensite. Second, it creates random local stresses that favor local strain order. Obviously, doping Co into the Ni-site of Ni-Co-Mn-Ga system satisfies these two conditions, which leads to the formation of strain glass. However, doping Co into the Mn or Ga site does not result in the formation of strain glass, because this causes the increase of martensitic stability of the system for the increase of e/a.[7] The driving force of martensite is strong enough to overcome the local barriers produced by the random local stresses of point defects and drives the system to transform into martensitic state. Comparing with the formation of normal strain glass, one more condition should be satisfied to generate ferromagnetic strain glass. That is, the point defect promotes the ferromagnetic exchange interaction in the system. It should be mentioned that it is not a necessary condition to require the pure martensitic terminal being ferromagnetic. This is because in some Heusler system the point defect that reinforces the ferromagnetic exchange interaction may generate the ferromagnetic transition at sufficient doping level,[24] despite its martensitic terminal is not ferromagnetic.

In conclusion, we found a ferromagnetic strain glass in $Ni_{55-x}Co_xMn_{20}Ga_{25}$ Heusler system by doping sufficient substitutional point defect Co into the Ni-site. The existence of ferromagnetic strain glass demonstrates that the short range strain ordering coexists with the long range magnetic moment ordering. The dopant Co in the Ni-site plays three fold roles: (1) suppressing the long range strain ordering, (2) promoting local strain ordering, and (3) enhancing the ferromagnetic exchange interaction in the Ni-Co-Mn-Ga system, which leads to the formation of ferromagnetic strain glass. The finding of ferromagnetic strain glass in Heusler system may lead to practical applications.

The present work was supported by the financial support under National Natural Science Foundation of China (Grant Nos. 51101118 and 51071117), National Basic Research Program of China (Grant Nos. 2012CB619401 and 2010CB631003), and the Fundamental Research Funds for Central Universities of China.

[1]K. Otsuka and X. Ren, Prog. Mater. Sci. **50**, 511 (2005).
[2]L. Mañosa, X. Moya, A. Planes, T. Krenke, M. Acet, and E. F. Wassermann, Mater. Sci. Eng. A **481–482**, 49 (2008).
[3]O. Heczko, J. Mag. Mag. Mater. **290–291**, 787 (2005).
[4]R. Kainuma, Y. Imano, W. Ito, Y. Sutou, H. Morito, S. Okamoto, O. Kitakami, K. Oikawa, A. Fujita, T. Kanomata, and K. Ishida, Nature (London) **439**, 957 (2006).
[5]A. Planes, L. Mañosa, and M. Acet, J. Phys.: Condens. Matter **21**, 233201 (2009).
[6]V. A. Chernenko, E. Cesari, V. V. Kokorin, and I. N. Vitenko, Scr. Metall. Mater. **33**, 1239 (1995).
[7]D. E. Soto-Parra, X. Moya, L. Mañosa, A. Planes, H. Flores-Zúñiga, F. Alvarado-Hernández, R. A. Ochoa-Gamboa, J. A. Matutes-Aquino, and D. Ríos-Jara, Philos. Mag. **90**, 2771 (2010).
[8]A. A. Cherechukin, T. Takagi, H. Miki, M. Matsumoto, and M. Ohtsuka, J. Appl. Phys. **95**, 1740 (2004).
[9]M. Todai, T. Fukuda, and T. Kakeshita, Mater. Trans. **51**, 906 (2010).
[10]Y. Zhou, D. Xue, X. Ding, Y. Wang, J. Zhang, Z. Zhang, D. Wang, K. Otsuka, J. Sun, and X. Ren, Acta Mater. **58**, 5433 (2010).
[11]Y. Zhou, D. Xue, X. Ding, K. Otsuka, J. Sun, and X. Ren, Appl. Phys. Lett. **95**, 151906 (2009).
[12]S. Sarkar, X. Ren, and K. Otsuka, Phys. Rev. Lett. **95**, 205702 (2005).
[13]Y. Wang, X. Ren, K. Otsuka, and A. Saxena, Phys. Rev. B **76**, 132201 (2007).
[14]Y. Wang, X. Ren, and K. Otsuka, Phys. Rev. Lett. **97**, 225703 (2006).
[15]V. A. Chernenko, C. Seguí, E. Cesari, J. Pons, and V. V. Kokorin, Phys. Rev. B **57**, 2659 (1998).
[16]C. Seguí, E. Cesari, J. Pons, and V. Chernenko, Mater. Sci. Eng. A **370**, 481 (2004).
[17]F. J. Pérez-Reche, E. Vives, L. Mañosa, and A. Planes, Phys. Rev. Lett. **87**, 195701 (2001).
[18]M. C. Gallardo, J. Manchado, F. J. Romero, J. del Cerro, E. K. H. Salje, A. Planes, and E. Vives, Phys. Rev. B **81**, 174102 (2010).
[19]S. Banik, R. Ranjan, A. Chakrabarti, S. Bhardwaj, N. P. Lalla, A. M. Awasthi, V. Sathe, D. M. Phase, P. K. Mukhopadhyay, D. Pandey, and S. R. Barman, Phys. Rev. B **75**, 104107(2007).
[20]B. Wedel, M. Suzuki, Y. Murakami, C. Wedel, T. Suzuki, D. Shindo, and K. Itagaki, J. Alloys Compd. **290**, 137(1999).
[21]Y. Ge, O. Heczko, O. Söderberg, and V. K. Lindroos, J. Appl. Phys. **96**, 2159 (2004).
[22]Y. Murakami, D. Shindo, M. Suzuki, M. Ohtsuka, and K. Itagaki, Acta Mater. **51**, 485 (2003).
[23]Z. Zhang, Y. Wang, D. Wang, Y. Zhou, K. Otsuka, and X. Ren, Phys. Rev. B **81**, 224102 (2010).
[24]D. Y. Cong, S. Roth, M. Pötschke, C. Hürrich, and L. Schultz, Appl. Phys. Lett. **97**, 021908 (2010).